Density of Liquid Niobium and Tungsten and the Estimation of Critical Point Data

M. LEITNER and G. POTTLACHER

Density as a function of temperature was measured for the liquid transition metals niobium and tungsten by means of ohmic pulse-heating. The generated data are extensively compared to the existing literature data, and the uncertainty is critically assessed according to the *guide to the expression of uncertainty in measurement* (GUM). Starting from the obtained liquid-phase density regression, the phase diagram, and the critical point, *i.e.*, critical temperature T_c and critical density ρ_c of niobium and tungsten are estimated. The so-obtained critical point for these two high-melting metals is compared to the data available in the existing literature.

https://doi.org/10.1007/s11661-019-05262-5
© The Author(s) 2019

I. INTRODUCTION

THE knowledge of a metal's density as a function of temperature is frequently crucial for many scientific considerations and technological applications. It is used as an input parameter in simulations that model thermal natural convection phenomena in furnaces and ladles, to calculate mass balance in refining operations or understand and model solidification processes, to name a few.[1,2] Density as a function of temperature is also needed for the calculation of thermal conductivity from thermal diffusivity and vice versa, or in the measurement of surface tension and viscosity. In fact, various models show a relatively strong sensitivity on input density data compared to other input-properties.[3] Density data of liquid transition metals, however, are often either scarcely available or are very inconsistent with each other. This is also a consequence of the high temperatures that are involved when dealing with liquid metals. These temperatures are typically above several thousand K for transition metals, which leads to a number of technical challenges. It is for this reason that a complementary revisit on liquid density data appears to be appropriate for several transition metals, such as niobium and tungsten.

The density of liquid metals is not only of direct technology-related interest, but also of fundamental scientific interest. Measuring a material's density as a function of temperature means that a part of this material's phase diagram is mapped in the temperature–density projection. Extending the measured density to higher temperatures leads the way to the material's critical point. For high melting metals, this unique point can be at extremely high temperatures well above 10,000 K and at extreme pressures of several hundred MPa. For this reason, the critical point of these metals can be reached experimentally only with great effort, if at all. However, measuring the liquid density at lower temperatures, *e.g.*, *via* ohmic pulse-heating, still allows extrapolating of the measured data points according to simplified theoretical models.[4] By this means one can give an estimation of the critical density, critical temperature and the material's phase diagram in the temperature–density projection. Critical point data of high-melting metals might even be useful one day in future ultra-high temperature technologies, such as for aerospace and energy applications.

This paper is organized as follows: Section II provides details on the experimental procedure and the ohmic pulse-heating setup is briefly explained. Section III presents and discusses the obtained temperature–resolved density data and gives the estimated phase diagrams of niobium and tungsten together with their critical point. In Section IV, uncertainties of the presented data are assessed.

II. EXPERIMENTAL PROCEDURE AND DATA EVALUATION

Wire-shaped W and Nb specimens with a diameter of 0.5 mm and a length of 40 mm were investigated using an ohmic pulse-heating apparatus (OPA) as described in Reference 5. Before the experiments, the specimens (niobium: Co. Advent, purity: 99.9 wt pct, catalog no.: NB537115, Gi1592, condition: temper annealed.

M. LEITNER and G. POTTLACHER are with the Institute of Experimental Physics, Graz University of Technology, NAWI Graz, Petersgasse 16, 8010 Graz, Austria. Contact e-mail: matthias.leitner@tugraz.at

Manuscript submitted November 30, 2018.
Article published online May 20, 2019

Tungsten: Co. Goodfellow, purity: 99.95 wt pct, catalog no.: W 005160/18, LS73129 J F, condition: clean) were treated with abrasive paper (grade 1200) and cleaned with acetone. Subsequently, the wire-samples were subjected to a strong current pulse. Within 45 μs (Nb) and 53 μs (W), the wires are thus heated from room temperature into the liquid phase until boiling sets in and the wire explodes.

During the experiment, the temperature and thermal expansion are recorded, as described in the following sections. The sample (surface) radiance is monitored by means of pyrometry to account for the short timescales. Simultaneously, a fast CCD-camera acquires images of the expanding wire at specific instants in time that can subsequently be related to a corresponding temperature. The experiments were conducted under an inert N_2 atmosphere with a slight static overpressure of about 1.5 bar.

A. *Temperature*

The surface radiance of the sample is monitored throughout the experiment by using a pyrometer with a central wavelength of $\lambda = 650\,\text{nm}$ and a full-width-at-half-maximum of 27 nm. Data points are collected every 100 ns. Neutral density filters were employed to break down the pyrometer signal by a constant fraction and thus enlarge the measurable temperature region. After concluding the experiment, the known radiance temperature at melting is assigned to the visible inflection in the thermogram, *i.e.*, the melting plateau, to derive a radiance temperature $T_r(t)$ as a function of time t. The radiance temperature at melting is for this purpose calculated using the literature value for the true melting temperature T_m and the normal spectral emissivity at melting ε_m. Together with the temperature-dependent normal spectral emissivity $\varepsilon(\lambda, T_r)$ of the metal, the pyrometer signal is then converted into a true temperature $T(t)$ following Eq. [1]:

$$T(t) = \frac{c_2}{\lambda \cdot \ln\left\{\varepsilon(\lambda, T_r) \cdot \left[\exp\left(\frac{c_2}{\lambda \cdot T_r(t)}\right) - 1\right] + 1\right\}}, \qquad [1]$$

where c_2 is the second radiation constant. Table I sums up the utilized values and parameters to derive the true temperature $T(t)$ for tungsten and niobium. For a more detailed description of the temperature deduction as well as an exemplary thermogram, please refer to a previous publication.[6]

B. *Thermal Radial Expansion and Density*

Thermal radial expansion is investigated by means of fast shadow-imaging. During the experiment, a high-power photoflash (*Multiblitz* X10, 1000 Ws) provides intense background illumination to produce shadow images of the expanding wire at specific instants in time. These instants are time-synchronized with the pulse-heating experiment. By this means, a temperature can be assigned to each shadow image taken. The CCD-camera system (Co. PCO imaging with controller unit by Co. Theta System and Graz Univ. of Technol.) is capable of acquiring one image every 2.5 μs, compare *e.g.*, References 6 and 7. After the experiment, summing over the pixel lines of each image gives a cup-shaped intensity profile. The full-width-at-half-maximum of these intensity profiles obtained by this means corresponds to the diameter d of the wire at a specific time and thus temperature T. In relating this temperature-dependent diameter $d(T)$ to the diameter at room temperature d_0, density can be derived by using the literature value for the room-temperature density ρ_0. Note that longitudinal expansion of the wire is inhibited thanks to the short timescales of the experiment. Thus, the measured relative radial expansion squared $(d(T)/d_0)^2$ equals the relative volume expansion $V(T)/V_0$ of the sample. The density as a function of temperature $\rho(T)$ can thus be calculated *via*

$$\rho(T) = \rho_0 \cdot \left(\frac{d_0}{d(T)}\right)^2. \qquad [2]$$

For niobium, we used a room-temperature density of $8.57 \times 10^3\,\text{kg m}^{-3}$ as given in the *CRC Handbook of Chemistry and Physics*.[8] For tungsten, a room-temperature density ρ_0 of $19256\,\text{kg m}^{-3}$ was adopted from Ming and Manghnani,[9] found in the *NIST Alloy data web application*.[10] Note that this density value is only 0.2 pct lower than that given in the *CRC Handbook of Chemistry and Physics*.[8]

C. *Critical Point Data*

The measured liquid-phase density as a function of temperature was taken to estimate the critical temperature T_c, critical density ρ_c , as well as the phase diagram in the (ρ,T)-plane. The estimation is done by an extrapolation algorithm following the method in the publication of Schröer and Pottlacher.[4] In this approach, the measured liquid-phase density is extrapolated according to simplified Ising- and mean-field behavior to estimate critical temperature and critical density.

Table I. Utilized Data for Temperature Deduction of the Metals Niobium and Tungsten

Metal	$\varepsilon(684.5\,\text{nm}, T_r)/1$	Validity Range	Melting Temperature T_m
Niobium	0.345	$2422 < T_r/\text{K} < 3700$	2745 K (2472 °C)
Tungsten	$0.4407 - 1.3916 \times 10^{-5}\,T_r$	$3207 < T_r/\text{K} < 4400$	3687 K (3414 °C)

Normal spectral emissivity ε at a wavelength of 684.5 nm as a function of radiance temperature T_r in K taken from Cagran *et al.*[33] Melting temperature T_m adopted from Bedford *et al.*[34]

A simplified phase diagram, given by the Eqs. [3] and [4], is then also constructed from the measured liquid-phase density $\rho_{+,\mathrm{meas}}(T)$ by extrapolating up to the critical temperature according to Eq. [3],

$$\rho_{\pm}(T) = \rho_{\mathrm{diam}} \pm b \cdot (T_c - T)^{1/3}\left(1 + b_2 \cdot (T_c - T)^{2/3}\right) . \quad [3]$$

In this equation, the subscript '+' indicates the saturated liquid line and '−' indicates the saturated vapor line of the phase diagram—the equation describes how the density changes as a function of temperature up to the critical point. ρ_{diam} is the so-called phase-diagram diameter, *i.e.*, the mean value between the saturated liquid density and the saturated vapor density at a given isotherm, $(\rho_+ + \rho_-)/2$. It is extrapolated up to the critical temperature T_c according to Eq. [4], where ρ_{diam} itself can be calculated from the measured liquid-phase density $\rho_{+,\mathrm{meas}}(T)$ that is located in the low-temperature branch of the binodal, *i.e.*, $\rho_{\mathrm{diam}} \approx \rho_{+,\mathrm{meas}}/2$,

$$\rho_{\mathrm{diam}}(T) = \rho_c\left(1 + a \cdot (T_c - T) + c \cdot (T_c - T)^{2/3}\right) . \quad [4]$$

The extrapolations described above yield the fitting coefficients b, b_2, a and c. For a more detailed description of the formalism, please refer to the original publication[4] or to a previous publication.[6]

Note, that this algorithm delivered remarkably good results when compared to experimentally obtained critical point data of the alkalis.[4] In addition, this approach was tested on the transition metal tantalum, which also delivered good concordance compared to the literature, see Reference 6.

III. RESULTS AND DISCUSSION

In this section, density as a function of temperature for the two metals niobium and tungsten is reported and discussed. From these data, the critical point as well as the phase diagram of the two metals are estimated.

A. *Density*

The measured liquid density of niobium and tungsten are plotted and compared to experimental data given in the literature. The liquid-phase density regressions are tabulated in Table II. The experimentally obtained data points are listed in Tables III (niobium) and IV (tungsten).

1. *Niobium*

Nine independent experiments were performed with niobium. The derived density is shown in Figure 1 together with literature values. At the beginning of the liquid phase, we obtain a density value of $\rho(T_{m,l}) = (7.69 \pm 0.09) \times 10^3\,\mathrm{kg\,m^{-3}}$, where the subscript 'l' indicates the liquid phase. This is in excellent agreement with the literature, but at a slightly lower value. Ishikawa *et al.*[11] report a value that is 0.5 pct higher, Gallob *et al.*[12] are higher by 0.7 pct, Hixson and Winkler by 0.4 pct,[13] Shaner *et al.* by approximately 1 pct.[14] Interestingly, the change of density with temperature shows significant inconsistency within the literature. While Paradis *et al.* are closest with an about 28 pct stronger density gradient, the deviation of the slope reported earlier by our group[12] is about 189 pct. However, the technique used then was a very simplistic shadowgraph method[7] which also delivered a seemingly higher thermal expansion with other metals.[15]

2. *Tungsten*

Figure 2 shows the density of tungsten as a function of temperature, derived from eight independent pulse-heating experiments. At melting, the density drops by approximately 5 pct to a value of $\rho(T_{m,l}) = (17.2 \pm 0.5) \times 10^3\,\mathrm{kg\,m^{-3}}$.

The data given in the literature appear to cluster into lower and higher density data. Allen[16] and Calverley[17] report a density at the beginning of melting, $\rho_{m,l}$, that is 1.9 and 2.4 pct higher than our value. The value given in the *CRC Handbook of Chemistry and Physics*[8] is also 2.4 pct higher than our value. Datapoints reported by Koval *et al.*[18] as well as Hess *et al.*[19] show very good agreement, both at the end of the solid phase and during the liquid phase. In particular, the data given by Koval *et al.* are in extraordinary agreement, while the data points given by Hess *et al.* start to deviate from our data at higher temperatures in the liquid phase. Data given by Paradis *et al.*[2] also agree reasonably well with our data. At the melting point, they deviate by 2.8 pct. For the sake of comparison, the density measured by Paradis *et al.* of an undercooled liquid W-droplet was extrapolated into the liquid phase.

The second set of data found in the literature (Seydel and Kitzel,[20] Berthault *et al.*,[21] Hixson and Winkler[22] as well as Hüpf *et al.*[23]) is significantly lower. At the beginning of the liquid phase, those authors report values that are between 4 pct (Hixson and Winkler) and 5.7 pct (Berthault *et al.*) lower than our value for $\rho(T_{m,l})$. Interestingly, the density data in the solid phase also show a somewhat unusual broad variation.

Table II. Fit-Coefficients for the Liquid-Phase Density of Niobium and Tungsten in the Form $\rho(T) = a - b \cdot T$. Uncertainty reported with a level of confidence 0.95 ($k = 2$)

Metal	$a/\mathrm{kg\,m^{-3}}$	$b/\mathrm{kg\,m^{-3}\,K^{-1}}$	Temperature Range	$U(\rho)/\rho$
Niobium	$(8.52 \pm 0.09) \times 10^3$	(0.304 ± 0.019)	$2745 \le T/\mathrm{K} \le 5847$	0.013 to 0.022
Tungsten	$(19.8 \pm 0.4) \times 10^3$	(0.71 ± 0.08)	$3687 \le T/\mathrm{K} \le 5631$	0.028 to 0.038

The relative density-uncertainty $U(\rho)/\rho$ at a fixed temperature T is given from the beginning of the liquid phase up to the highest temperature measured.

Table III. Niobium: Experimental Values of Density as a Function of Temperature $\rho(T)$ Derived from Thermal Expansion Measurements

T/K	T/°C	$\rho(T)$/kg m^{-3}	T/K	T/°C	$\rho(T)$/kg m^{-3}	T/K	T/°C	$\rho(T)$/kg m^{-3}
1983	1710	8307	2747	2474	7766	3589	3316	7465
2006	1733	8159	2750	2477	7788	3620	3347	7374
2057	1784	8252	2751	2478	7884	3670	3397	7363
2151	1878	8103	2764	2491	7635	3702	3429	7331
2175	1902	8202	2771	2498	7704	3931	3658	7428
2232	1959	8199	2774	2501	7677	3948	3675	7355
2300	2027	8175	2792	2519	7747	3957	3684	7358
2368	2095	8052	2870	2597	7766	4027	3754	7406
2417	2144	8154	2871	2598	7625	4068	3795	7301
2460	2187	7897	2911	2638	7609	4086	3813	7257
2475	2202	7995	3015	2742	7482	4120	3847	7248
2607	2334	8011	3024	2751	7649	4132	3859	7270
2618	2345	7965	3107	2834	7590	4199	3926	7342
2639	2366	7905	3135	2862	7471	4447	4174	7288
2705	2432	8048	3156	2883	7586	4453	4180	7180
2719	2446	7769	3160	2887	7439	4462	4189	7210
2726	2453	7858	3279	3006	7412	4687	4414	6993
2732	2459	7867	3400	3127	7530	4742	4469	7186
2736	2463	7809	3435	3162	7422	4997	4724	6937
2740	2467	7925	3462	3189	7530	5005	4732	7096
2741	2468	7873	3582	3309	7367	5797	5524	6664
2747	2474	7889	3584	3311	7560	5848	5575	6672

The density values were obtained with a room-temperature density of $\rho_0 = 8570\,\text{kg m}^{-3}$.[8]

Combined expanded temperature uncertainty for the liquid phase [$T > 2745$ K (2472 °C)]: $U_c(T)/T = 0.015$ at the beginning of the liquid phase up to $U_c(T)/T = 0.026$ at the highest temperature measured. Combined expanded density–uncertainty $U_c(\rho)/\rho = 0.013$. Uncertainties reported with a level of confidence 0.95 ($k = 2$).

Table IV. Tungsten: Experimental Values of Density as a Function of Temperature $\rho(T)$ Derived from Thermal Expansion Measurements

T/K	T/°C	$\rho(T)$/kg m^{-3}	T/K	T/°C	$\rho(T)$/kg m^{-3}	T/K	T/°C	$\rho(T)$/kg m^{-3}
2296	2023	18,697	3680	3407	17,867	3981	3708	17,105
2334	2061	18,734	3680	3407	17,619	4105	3832	16,863
2401	2128	18,939	3681	3408	17,658	4149	3876	17,171
2414	2141	18,708	3681	3408	18,207	4191	3918	17,026
2564	2291	18,755	3684	3411	17,974	4275	4002	16,561
2605	2332	18,765	3684	3411	17,738	4352	4079	16,870
2749	2476	18,670	3685	3412	18,072	4364	4091	16,734
2772	2499	18,555	3687	3414	17,524	4420	4147	16,418
2774	2501	18,498	3687	3414	18,076	4546	4273	16,774
2918	2645	18,640	3689	3416	17,571	4642	4369	16,223
3001	2728	18,697	3690	3417	17,579	4766	4493	16,442
3121	2848	18,581	3691	3418	17,301	4862	4589	16,100
3192	2919	18,509	3693	3420	17,779	4892	4619	16,477
3302	3029	18,491	3698	3425	17,165	4926	4653	16,178
3336	3063	18,164	3701	3428	17,287	4981	4708	15,873
3351	3078	18,343	3767	3494	17,052	5192	4919	16,358
3458	3185	18,267	3828	3555	17,205	5438	5165	15,959
3556	3283	18,261	3847	3574	16,989	5631	5358	16,080
3663	3390	18,008	3904	3631	16,849			

The density values were obtained with a room-temperature density of $\rho_0 = 19256\,\text{kg m}^{-3}$.[9]

Combined expanded temperature uncertainty for the liquid phase [$T > 3687$ K (3414 °C)]: $U_c(T)/T = 0.018$ at the beginning of the liquid phase up to $U_c(T)/T = 0.025$ at the highest temperature measured. Combined expanded density-uncertainty $U_c(\rho)/\rho = 0.013$. Uncertainties reported with a level of confidence 0.95 ($k = 2$).

B. *Critical Point Data*

The critical point of niobium and tungsten was estimated according to the publication of Schröer and Pottlacher.[4] Starting from the critical temperature T_c and critical density ρ_c, the phase diagram was estimated as described in Section II–C. Table V gives the parameters needed to plot these phase diagrams in the (ρ, T)-plane. On the way to estimate the phase diagram, a simplified Ising

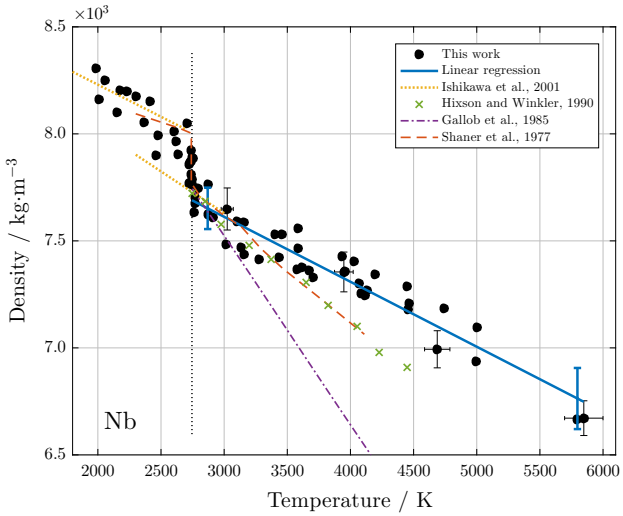

Fig. 1—Density of niobium as a function of temperature. The vertical dashed line marks the melting point. Full circles and solid line: Experimental data obtained during this work and corresponding liquid-phase linear regression. Uncertainties given at a 95 pct confidence level ($k = 2$).

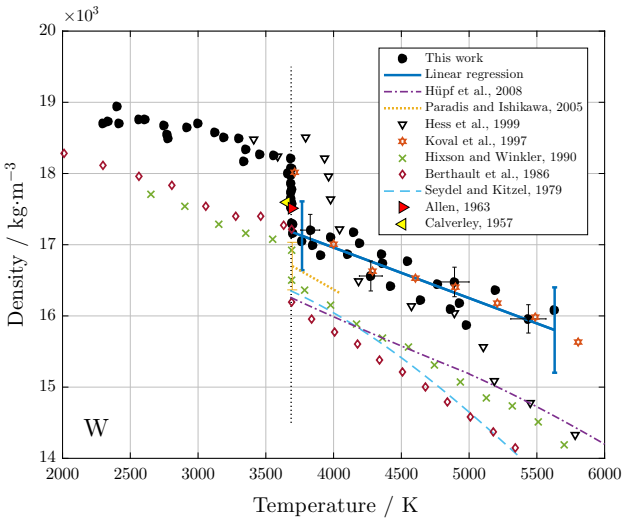

Fig. 2—Density of tungsten as a function of temperature. The vertical dotted line indicates the melting point. Full circles and solid line: This work's experimental data and corresponding liquid-phase linear regression. Uncertainties given at a 95 pct confidence level ($k = 2$). In this plot, data of Paradis *et al.*[2] were extrapolated into the liquid phase.

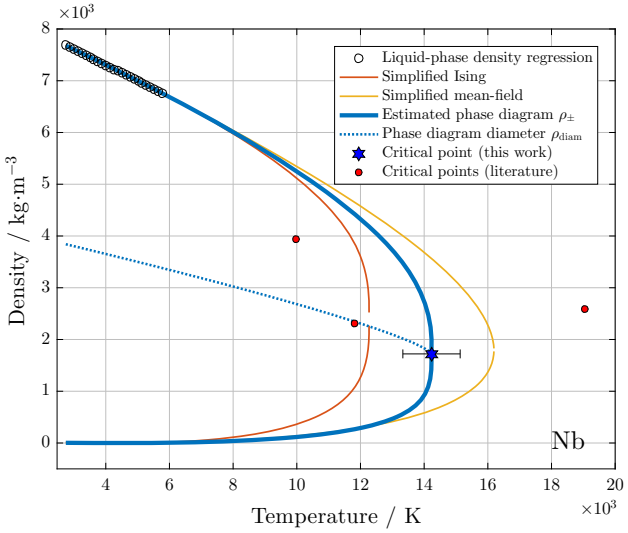

Fig. 3—Niobium: Estimated phase diagram (thick solid line) with nonlinear diameter (dotted line) and critical point (star). Open circles: Data generated by the linear regression of this work's experimental density data. Thin solid lines: Phase diagrams according to a simplified mean-field and Ising behavior. Literature values for the critical point are given (red circles) (Color figure online).

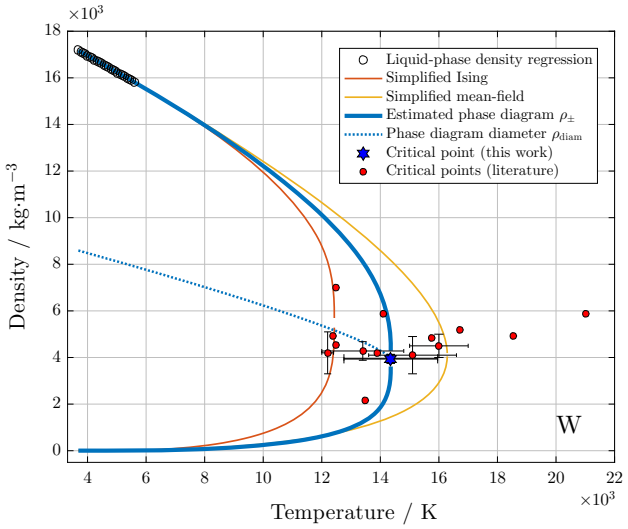

Fig. 4—Tungsten: Estimated phase diagram (thick solid line) with nonlinear diameter (dotted line) and critical point (star). Open circles: Data generated by the linear regression of this work's experimental density data. Thin solid lines: Phase diagrams according to a simplified mean-field and Ising behavior. Literature values for the critical point are given (red circles) (Color figure online).

Table V. Parameters of the Estimated Phase Diagram of Niobium and Tungsten According to Eqs. [3] and [4]

Metal	ρ_c/kg m^{-3}	T_c/K	$a/10^{-5}$K^{-1}	$c/10^{-3}$ K$^{-2/3}$	$b/10^{-1}$ K$^{-1/3}$	$b_2/10^{-4}$ K$^{-2/3}$
Niobium	1722	14,231	4.42	1.42	1.47	3.13
Tungsten	3945	14,357	4.50	1.43	3.38	3.16

Temperature range of validity from melting temperature T_m up to the critical temperature T_c of the respective metal. a, c, b and b_2 are the obtained fitting coefficients, ρ_c is the critical density.

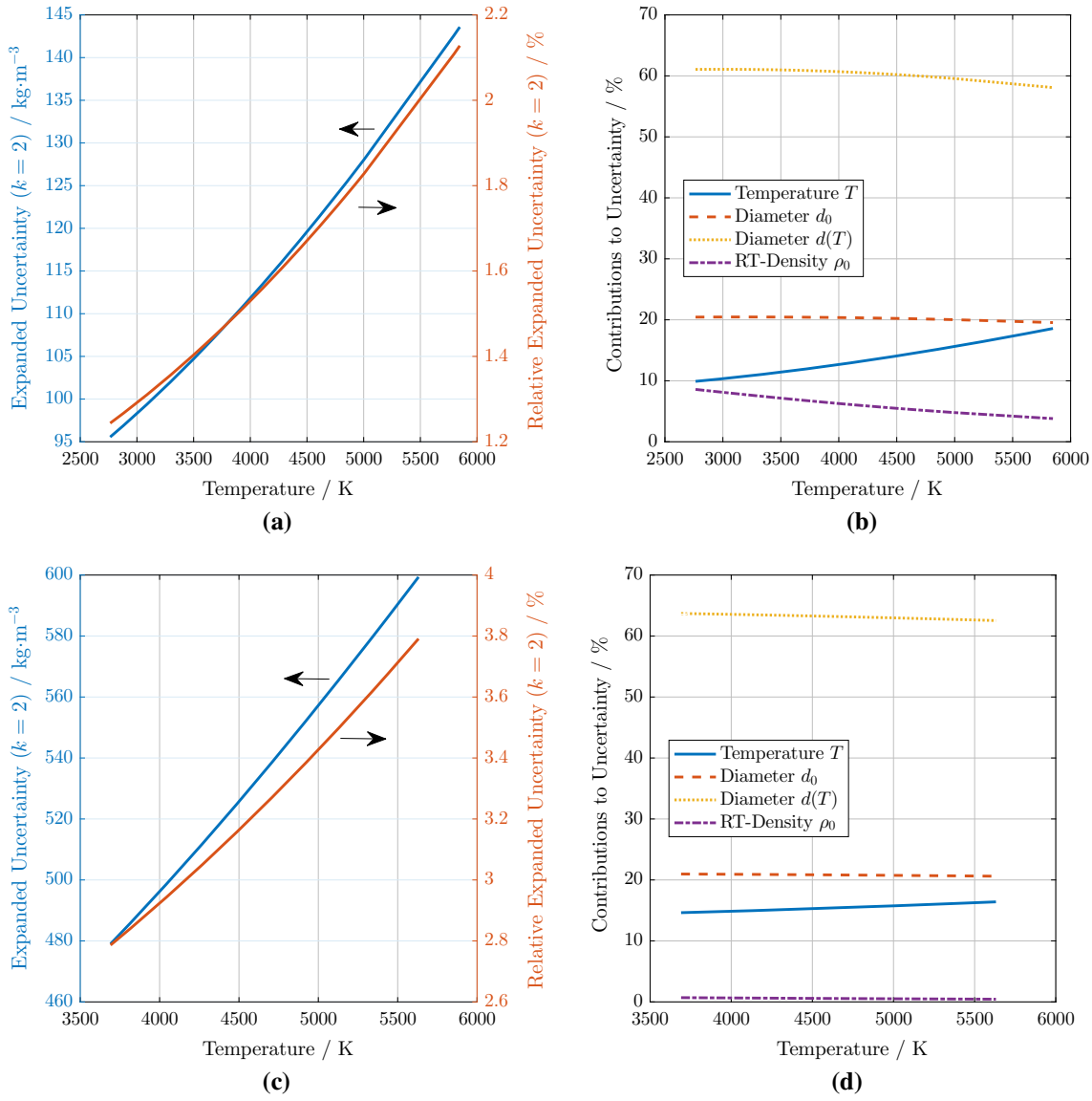

Fig. 5—Uncertainty of the liquid-phase density-regression estimated according to the GUM. Expanded uncertainty and relative expanded uncertainty ($k = 2$) as a function of temperature for niobium (*a*) and tungsten (*c*). Uncertainty budget as a function of temperature for niobium (*b*) and tungsten (*d*).

and mean-field approach is used, compare Reference 4. The resulting phase diagrams are also plotted in Figures 3 and 4. In addition, (T_c, ρ_c)-pairs were plotted when found in the literature, see Minakov *et al.*[24] as well as Hess and Schneidenbach.[25]

1. *Niobium*

For niobium, the extrapolation yields a critical point of

$$T_{c,Nb} = (14.2 \pm 0.9) \times 10^3\ \mathrm{K}$$
$$\rho_{c,Nb} = (1.72 \pm 0.05) \times 10^3\ \mathrm{kg\,m^{-3}}.$$

The estimated phase diagram is depicted in Figure 3 together with data reported in the literature. Data in the literature show a wide range from $T_c = 9989$ K reported by Young[26] to values as high as $T_c = 19{,}580$ K, published by Lang.[27] Compared to these literature values, and to the summarized values found in the comprehensive summaries on critical point data given by Blairs and Abbasi[28] and Hess and Schneidenbach,[25] our value for the critical temperature is located in the middle range.

Data for the critical density range from $2.32 \times 10^3\ \mathrm{kg\,m^{-3}}$ as reported by Hess and Schneidenbach[25] to $3.94 \times 10^3\ \mathrm{kg\,m^{-3}}$, published by Young.[26] The critical density reported by us is the lowest value among those found in the literature.

2. *Tungsten*

Figure 4 shows the estimated phase diagram and critical point of tungsten. The evaluation yields a critical point of

$$T_{c,W} = (14.4 \pm 1.6) \times 10^3\ \mathrm{K}$$
$$\rho_{c,W} = (3.95 \pm 0.19) \times 10^3\ \mathrm{kg\,m^{-3}}.$$

Plenty of previous considerations on the critical point can be found in the literature. The reported values range from $T_c = 7650$ K, published by Blairs and Abbasi[29] to values as high as $T_c = 23{,}000$ K, reported by Grosse.[30] Comparing our value to the multitude of predictions listed by Minakov *et al.*[24] and Blairs and Abbasi[28,29] shows that our critical temperature is in the lower middle range of reported literature values. The same is true for our critical density prediction; it is also in the lower middle range compared to the literature.

IV. UNCERTAINTIES

Uncertainties for the experimental density values were calculated according to the *guide to the expression of uncertainty in measurement*, shortly referred to as GUM.[31] The uncertainty of the regression coefficients are also calculated according to GUM, by including the individual datapoint uncertainties in x- and y- directions.[32] As a result, Figures 5(a) and (c) show the expanded density uncertainty at a 95 pct confidence level at a given temperature T, *i.e.*, the temperature uncertainty is converted into a density uncertainty *via* the slope of the density regression. We discussed the approach in more detail in our previous publication on tantalum.[6] For the room-temperature density uncertainty, we adopted $u(\rho_{0,\mathrm{Nb}}) = 14\,\mathrm{kg\,m^{-3}}$ and $u(\rho_{0,\mathrm{W}}) = 20\,\mathrm{kg\,m^{-3}}$ from Reference 9. Figures 5(b) and (d) show the temperature-resolved uncertainty budget for the two investigated metals.

An uncertainty for the critical point was estimated by using the uncertainties of the density fit-coefficients listed in Table II. The extrapolation procedure was not only conducted for $\rho = a + b \cdot T$, but also for $\rho = (a + |u(a)|) + (b + |u(b)|) \cdot T$ and $\rho = (a - |u(a)|) + (b - |u(b)|) \cdot T$, where $b < 0$ and $u(x)$ denotes the standard uncertainty of x ($k = 1$). The doubled standard deviation of the mean value of these three critical point results is reported as uncertainty. Note that this uncertainty therefore only gives a rough idea of how much the critical point can vary due to the uncertainty of the density fit.

V. CONCLUSION

The temperature-dependent density of liquid niobium and liquid tungsten were determined using the ohmic pulse-heating technique. In our experiments, the obtained density gradient of liquid niobium turned out to be lower than the various different values reported in the literature, while the density at the beginning of the liquid phase is in very good agreement with the data from the literature comparison. For tungsten, the situation is different. Here, the density gradient fits in well with reported literature values, but there is a shift to lower density values of up to 5.7 pct at the beginning of the liquid phase for some authors. Others report values at melting that are up to 2.4 pct higher.

The obtained density–temperature relationship was used to estimate a phase diagram and the critical temperature in addition to the critical density of niobium and tungsten. Comparing the obtained values to the literature shows that our values for the critical temperatures of niobium and tungsten are in the (lower) middle range of the reported values. Our estimate for the critical density turned out to be at the lower end of those found in the literature.

ACKNOWLEDGMENTS

Open access funding provided by Graz University of Technology. We would like to thank Dan Alexandru Opris for the laboratory assistance during the tungsten measurements.

OPEN ACCESS

This article is distributed under the terms of the Creative Commons Attribution 4.0 International License (http://creativecommons.org/licenses/by/4.0/), which permits unrestricted use, distribution, and reproduction in any medium, provided you give appropriate credit to the original author(s) and the source, provide a link to the Creative Commons license, and indicate if changes were made.

REFERENCES

1. T. Iida and R. Guthrie: *The Physical Properties of Liquid Metals*, Clarendon Press, Oxford, 1988, p. 47.
2. P.-F. Paradis, T. Ishikawa, R. Fujii, and S. Yoda: *Appl. Phys. Lett.*, 2005, vol. 86 (4), p. 041901.
3. P. Quested, R. Morrell, A. Dinsdale, and L. Chapman : *High Temp. - High Press.*, 2018, vol. 47, pp. 365–77.
4. W. Schröer and G. Pottlacher: *High Temp. - High Press.*, 2014, vol. 43, pp. 201–15.
5. E. Kaschnitz, G. Pottlacher, and H. Jäger: *Int. J. Thermophys.*, 1992, vol. 13 (4), pp. 699–710.
6. M. Leitner, W. Schröer, and G. Pottlacher: *Int. J. Thermophys.*, 2018, vol. 39 (11), p. 124.
7. G. Pottlacher and T. Hüpf: *Thermal Conductivity 30/Thermal Expansion 18*, DEStech Publications, Inc., 2010, pp. 192–206.
8. W.M. Haynes, ed.: *CRC Handbook of Chemistry and Physics*, 96th ed., CRC Press, 2015–2016.
9. L.C. Ming and M.H. Manghnani: *J. Appl. Phys.*, 1978, vol. 49 (1), pp. 208–12.
10. O. Database: NIST Alloy Data web application: 2018, https://trc.nist.gov/metals_data/. Accessed Oct 2018.
11. T. Ishikawa, P.-F. Paradis, and T. Itami: *Meas. Sci. Technol.*, 2005, vol. 16, pp. 443–51.
12. R. Gallob, H. Jäger, and G. Pottlacher: *High Temp. - High Press.*, 1985, vol. 17, pp. 207–13.
13. R. Hixson and M. Winkler: *High Press. Res.*, 1990, vol. 4, pp. 555–57.
14. J.W. Shaner, G.R. Gathers, and W.M. Hodgson: *Proceedings of the Seventh Symposium on Thermophysical Properties*, A. Cezailiyan, ed., American Society of Mechanical Engineers, Gaithersburg, Maryland, May 10–12, 1977, pp. 896–903.
15. G. Pottlacher, T. Neger, and H. Jäger: *Int. J. Thermophys.*, 1986, vol. 7 (1), pp. 149–59.

16. B. Allen: *Trans. AIME*, 1963, vol. 227 (239), p. 47.
17. A. Calverley: *Proc. Phys. Soc., Sect. B*, 1957, vol. 70 (11), p. 1040.
18. S.V. Koval, N.I. Kuskova, and S.I. Tkachenko: *High Temp.*, 1997, vol. 35 (6), pp. 863–66.
19. H. Hess, A. Kloss, A. Rakhel, and H. Schneidenbach: *Int. J. Thermophys.*, 1999, vol. 20 (4), pp. 1279–88.
20. U. Seydel and W. Kitzel: *J. Phys. F: Metal Phys.*, 1979, vol. 9 (9), pp. L153–L160.
21. A. Berthault, L. Arles, and J. Matricon: *Int. J. Thermophys.*, 1986, vol. 7 (1), pp. 167–79.
22. R. Hixson and M. Winkler: *Int. J. Thermophys.*, 1990, vol. 11 (4), pp. 709–18.
23. T. Hüpf, C. Cagran, G. Lohöfer, and G. Pottlacher: *J. Phys.: Conf. Ser.*, 2008, vol. 98 (6), p. 062002.
24. D.V. Minakov, M.A. Paramonov, and P.R. Levashov: *Phys. Rev. B*, 2018, vol. 97, p. 024205.
25. H. Hess and H. Schneidenbach: *Z. Metallkd.*, 1996, vol. 87, pp. 979–84.
26. D.A. Young: *A Soft-Sphere Model For Liquid Metals*, Tech. rep., Lawrence Livermore Laboratory, Livermore, 1977.
27. G. Lang: *Z. Metallkd.*, 1977, vol. 68 (3), pp. 213–18.
28. S. Blairs and M.H. Abbasi: *J. Colloid Interface Sci.*, 2006, vol. 304 (2), pp. 549–53.
29. S. Blairs and M.H. Abbasi: *Acustica*, 1993, vol. 79, pp. 64–72.
30. A. Grosse: *J. Inorg. Nucl. Chem.*, 1961, vol. 22 (1–2), pp. 23–31.
31. W.G. of the Joint Committee for Guides in Metrology (JCGM/WG 1): *Evaluation of measurement data—Guide to the expression of uncertainty in measurement*, JCGM—Joint Committee for Guides in Metrology, 2008.
32. M. Matus: *Tech. Mess.*, 2005, vol. 72, pp. 584–91.
33. C. Cagran, C. Brunner, A. Seifter, and G. Pottlacher: *High Temp. - High Press.*, 2002, vol. 34 (6), pp. 669–79.
34. R. Bedford, G. Bonnier, H. Maas, and F. Pavese: *Metrologia*, 1996, vol. 33, pp. 133–54.

Publisher's Note Springer Nature remains neutral with regard to jurisdictional claims in published maps and institutional affiliations.